frontiers in Chemistry

ORIGINAL RESEARCH
published: 19 March 2019
doi: 10.3389/fchem.2019.00122

Rational Design of Low-Band Gap Star-Shaped Molecules With 2,4,6-Triphenyl-1,3,5-triazine as Core and Diketopyrrolopyrrole Derivatives as Arms for Organic Solar Cells Applications

Xinhao Zhang [1,2] *and Ruifa Jin* [1,2]*

[1] *Inner Mongolia Key Laboratory of Photoelectric Functional Materials, Chifeng University, Chifeng, China,* [2] *College of Chemistry and Chemical Engineering, Chifeng University, Chifeng, China*

OPEN ACCESS

Edited by:
Doo Soo Chung,
Seoul National University, South Korea

Reviewed by:
Sungu Hwang,
Pusan National University, South Korea
Ahmad Irfan,
King Khalid University, Saudi Arabia

***Correspondence:**
Ruifa Jin
ruifajin@163.com

Specialty section:
This article was submitted to Physical Chemistry and Chemical Physics, a section of the journal Frontiers in Chemistry

Received: *04 December 2018*
Accepted: *15 February 2019*
Published: *19 March 2019*

Citation:
Zhang X and Jin R (2019) Rational Design of Low-Band Gap Star-Shaped Molecules With 2,4,6-Triphenyl-1,3,5-triazine as Core and Diketopyrrolopyrrole Derivatives as Arms for Organic Solar Cells Applications. Front. Chem. 7:122. doi: 10.3389/fchem.2019.00122

A series of D–A novel star-shaped molecules with 2,4,6-triphenyl-1,3,5-triazine (TPTA) as core, diketopyrrolo[3,4-c]pyrrole (DPP) derivatives as arms, and triphenylamine (TPA) derivatives as end groups have been systematically investigated for organic solar cells (OSCs) applications. The electronic, optical, and charge transport properties were studied using density functional theory (DFT) and time-dependent DFT (TD-DFT) approaches. The parameters such as energetic driving force ΔE_{L-L}, adiabatic ionization potential *AIP*, and adiabatic electron affinity *AEA* were also calculated at the same level. The calculated results show that the introduction of different groups to the side of DPP backbones in the star-shaped molecules can tune the frontier molecular orbitals (FMOs) energy of the designed molecules. The designed molecules can provide match well with those of typical acceptors PCBM ([6,6]-phenyl-C61-butyric acid methyl ester) and PC71BM ([6,6]-phenyl-C71-butyric acid methyl ester). Additionally, the absorption wavelengths of the designed molecules show bathochromic shifts compared with that of the original molecule, respectively. The introduction of different groups can extend the absorption spectrum toward longer wavelengths, which is beneficial to harvest more sunlight. The calculated reorganization energies suggest that the designed molecules are expected to be the promising candidates for ambipolar charge transport materials except molecule with benzo[c]isothiazole group can be used as hole and electron transport material. Moreover, the different substituent groups do not significantly affect the stability of the designed molecules.

Keywords: star-shaped molecules, diketopyrrolopyrrole derivatives, optical and electronic properties, frontier molecular orbitals (FMOs), organic solar cells (OSCs)

INTRODUCTION

Nowadays, organic π-conjugated small molecules (SMs) used as the donors in organic solar cells (OSCs) have drawn intense attention because of their outstanding advantages, such as excellent reproducibility, easy purification, well-defined chemical and optoelectronic properties (Coughlin et al., 2014; Yao et al., 2016; Bin et al., 2017). Owing to the tremendous efforts on improving the performance of OSCs based on SMs, their power conversion efficiency (PCE) has surpassed over 10% recently (Zhou et al., 2012; Kan et al., 2015). However, it is worth noting that their overall performance still falls behind that of their polymer counterparts (Ni et al., 2013; Lin and Zhan, 2016). Accordingly, to address this issue, it is a big challenge to design and synthesize high-performance and desirable donor novel SMs (Chaudhry et al., 2018; Irfan et al., 2018; Wazzan et al., 2018). In general, the high-efficiency SMs donor materials should possess suitable frontier molecular orbital (FMOs) (including the highest occupied molecular orbital, HOMO, and lowest unoccupied molecular orbital, LUMO) energy levels, high charge carrier mobility, broad absorption region, and miscibility with fullerene derivatives. In this regard, the HOMO level of the designed donor materials should been reduced to increase the open circuit voltage (V_{oc}), because the HOMO of donor and the LUMO of acceptor are closely relate to the V_{oc}. With the aim to harvest more sunlight, the energy gaps of the designed donor materials should been decreased, which results in an increase in the short circuit current density (J_{sc}) (Loser et al., 2017; Maglione et al., 2017; Zhang et al., 2017). Moreover, a key factor that impact on the efficient exciton splitting and charge dissociation is the downhill energetic driving force (ΔE_{L-L}), which is the energy differences between the LUMOs of the donor and acceptor. The ΔE_{L-L} value should be about 0.3 eV to ensure efficient charge transfer, exciton splitting, and charge dissociation (Scharber et al., 2006). Therefore, an ideal donor material should have narrowing the HOMO-LUMO gap (E_g) and suitable FMOs energy levels with PCBM ([6,6]-phenyl-C61-butyric acid methyl ester) and PC71BM ([6,6]-phenyl-C71 butyric acid methyl ester), which are widely employed as acceptors in OSCs (He et al., 2007; Lenes et al., 2008). Among the various approaches to design organic π-conjugated SMs materials with the long range absorption, one of the successful approaches is to incorporate the electron-donating (D) and electron-accepting (A) moieties in π-conjugated SMs (Qu and Tian, 2012; Guo et al., 2017; Wang et al., 2017). The FMOs energy levels, absorption and emission properties as well as intermolecular charge transfer of these materials can be tuned effectively by altering the chemistries of the donor and acceptor units. At the same time, adjusting the donor and acceptor units can also affect their self-assembly in the solid state. Among the various D–A type SMs donors for OSCs, diketopyrrolo[3,4-c]pyrrole (DPP)-based molecules are promising building blocks owing to their excellent coplanarity, broader absorption region, and thermal stability (Chen et al., 2013; Lin et al., 2013; Zhang et al., 2014). Furthermore, the introduction of the planar heteroarenes into the strong electron-withdrawing DPP-based molecules backbones can lead to lower the band gap because of increasing effective conjugation length (Dutta et al., 2012; Patra et al., 2013). In addition, star-shaped SMs materials with π-conjugated arms can harvest sunlight effectively because of their extended dimensionality. Meanwhile, their steric hindrances can prevent the formation of an ordered, long-range, and coplanar π-π stacking, which are beneficial for their charge transport property (Irfan et al., 2017). Therefore, the star-shaped D–A type DPP-based molecules may possess narrower band gap, broader absorption region, strong light absorption, and high charge carrier mobility (Sharma et al., 2014; Shiau et al., 2015).

Considering these merits and characteristics mentioned above, in this contribution, we report the design of a series of novel star-shaped DPP-based molecules with electron-accepting 2,4,6-triphenyl-1,3,5-triazine (TPTA) as core, electron accepting DPP derivatives as arms, and electron-donating triphenylamine derivatives (TPA) as end groups for OSCs applications (as shown in **Scheme 1**). With the aim to investigate the relationships between structure and properties of the designed molecules, the different planar heteroarenes have been introduced into the side of DPP molecules backbones in the star-shaped molecules. The HOMO energy (E_{HOMO}), LUMO energy (E_{LUMO}), HOMO–LUMO gap (E_g), energetic driving force ΔE_{L-L}, and absorption spectra of the designed molecules were systematically investigated by applying density functional theory (DFT) and time-dependent DFT (TD-DFT) methodology. The charge transfer properties (reorganization energy, λ) were also simulated.

COMPUTATIONAL DETAILS

Using the Gaussian 09 W software package (Frisch et al., 2009), all the geometry optimizations and frequency for the designed molecules in the gas phase were performed with the DFT method. No imaginary frequency was used to ensure the nature of the stationary point for the optimized molecules. On the basis of the optimized structures, the absorption spectra of the designed molecules were predicted using the TD-DFT method. The 6-31G (d,p) basis set was employed for all calculations in this work. For the FMOs energy levels of the designed molecules, because it is difficult to describe the virtual orbitals theoretically (Wu et al., 2013). The LUMO energy levels can be calculated with the equation, $E_{LUMO} = E_{HOMO} + E^{ex}$, where E^{ex} represents the first vertical excited energy (Zhang and Musgrave, 2007; Ku et al., 2011; Zhang et al., 2012). A crucial step in the theoretical investigations is to select an appropriate exchange correlation functional. With the aim to select an appropriate approach, we chose various functionals such as B3LYP (Lee et al., 1988), PBE0 (Adamo and Barone, 1999), LC-wPBE (Tawada et al., 2004), M062X (Zhao and Truhlar, 2008), and CAM-B3LYP (Yanai et al., 2004) to optimize the geometries of the parent molecule **1**. Based on the optimized geometries, the absorptions were predicted using the TD-DFT method. The longest wavelengths of absorption (λ_{abs}) as well as the experimental data are shown in **Figure 1**. As showing **Figure 1**, the calculated λ_{abs} value obtained at PBE0 (543 nm) level provided better agreement with the experimental value (523 nm) (Shiau et al., 2015) than those obtained with other levels of theory, with the deviation being 20 nm. Although B3LYP appeared adapted to 1,3,5-triazine and

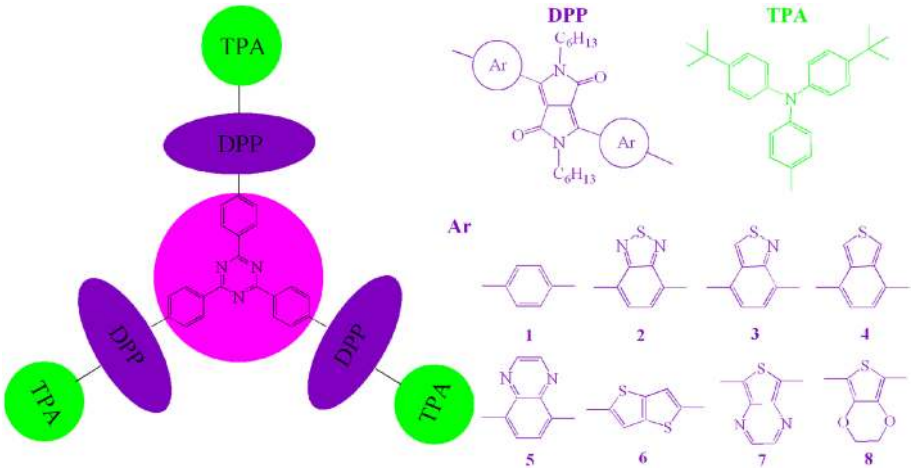

SCHEME 1 | Molecule models of **1**–**8** investigated in this work.

DPP derivatives in literature (Feng et al., 2014; Vala et al., 2014; Jin, 2015; Jin and Irfan, 2015; Jin and Xiao, 2015; Fujii et al., 2016), the λ_{abs} value obtained at the B3LYP/6-31G (d,p) level is worsen accordance with the experimental data (the deviation is 48 nm) than that for at the PBE0/6-31G (d,p) level (the deviation is 20 nm). Additionally, we also calculated the FMOs energy levels of molecule **1** using both at PBE0 and B3LYP methods. The calculated E_{HOMO} and E_{LUMO} values (−5.04 and −2.76 eV) at the PBE0/6-31G (d,p) level are more close to the electrochemical measurements data (−5.47 and −3.41 eV) (Shiau et al., 2015) than those obtained at the B3LYP/6-31G (d,p) level (−4.82 and −2.67 eV), respectively. Furthermore, in order to make further investigation of the validity of the selected approach, both PBE0 and B3LYP methods were also employed to optimize the structure of PCBM and PC71BM. The calculated E_{HOMO} and E_{LUMO} of PCBM and PC71BM along with available experimental data are listed in **Table S1**. Inspection of **Table S1** reveals clearly that the E_{HOMO} and E_{LUMO} at the PBE0/6-31G (d,p) level of PCBM are −5.98 and −3.99 eV, and the corresponding values of PC71BM are −5.92 and −3.82 eV, respectively. These are well reproduce the experimental values of PCBM (−6.00 and −3.80 eV) (Jeon et al., 2016) and PC71BM (−6.00 and −3.95 eV) (Chandrasekharam et al., 2014), respectively. However, at B3LYP/6-31G (d,p) level, the calculated E_{HOMO} and E_{LUMO} of PCBM are −5.67 and −3.75 eV, while the corresponding values of PC71BM are −5.61 and −3.60 eV, respectively. It was noticed that B3LYP overestimate the E_{HOMO} and E_{LUMO} of PCBM and PC71BM. The B3LYP overestimate the E_{HOMO} and E_{LUMO} compared with experimental value, as reported in the literature (Blouin et al., 2008; Xiao et al., 2010; Abbotto et al., 2012). Therefore, PBE0 functional is reasonable to investigate the current system. In order to obtain insight into the method to describe and the influence of functionals on the optical properties, the absorption spectrum of the designed molecules were also simulated at B3LYP/6-31G (d,p) levels.

It is well-known that the reorganization energy (λ) play the dominant role in the effective charge transfer according to the Marcus theory (Marcus, 1964, 1993). A good charge transfer materials should possess lower λ values, which led to higher charge transfer rate. We only pay attention to the internal reorganization energy in this work owing to the low dielectric constant of medium in OSCs materials (Marcus, 1964). The electron (λ_e) and hole (λ_h) reorganization energy can be expressed as follows (Köse et al., 2007; Sancho-García, 2007):

$$\lambda e = \left(E_0^- - E_-^-\right) + \left(E_-^0 - E_0^0\right) \quad (1)$$

$$\lambda h = \left(E_0^+ - E_+^+\right) + \left(E_+^0 - E_0^0\right) \quad (2)$$

Here, $E_0^{\pm}$ and $E_{\pm}^{\pm}$ are the energies of the cationic (anionic) states with the optimized neutral and cationic (anionic) geometry, respectively. $E_{\pm}^0$ and E_0^0 represent the energy of the neutral states with the optimized geometry of the cationic (anionic) and neutral structures, respectively. The λ_e and λ_h of the designed molecules were predicted at the PBE0/6-31G(d,p) level.

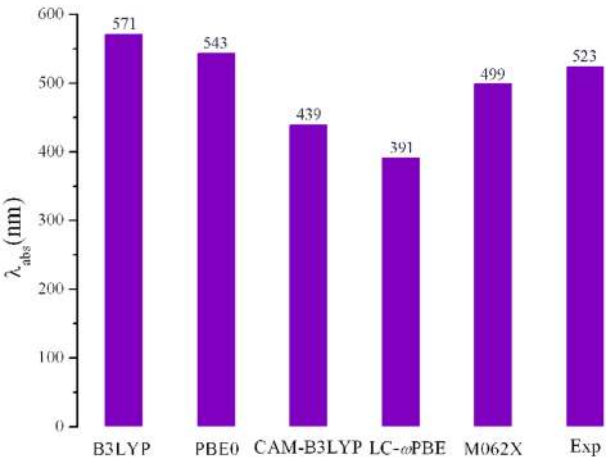

FIGURE 1 | Calculated absorption wavelengths (λ_{abs}) of **1** using various functionals, together with the experimental result.

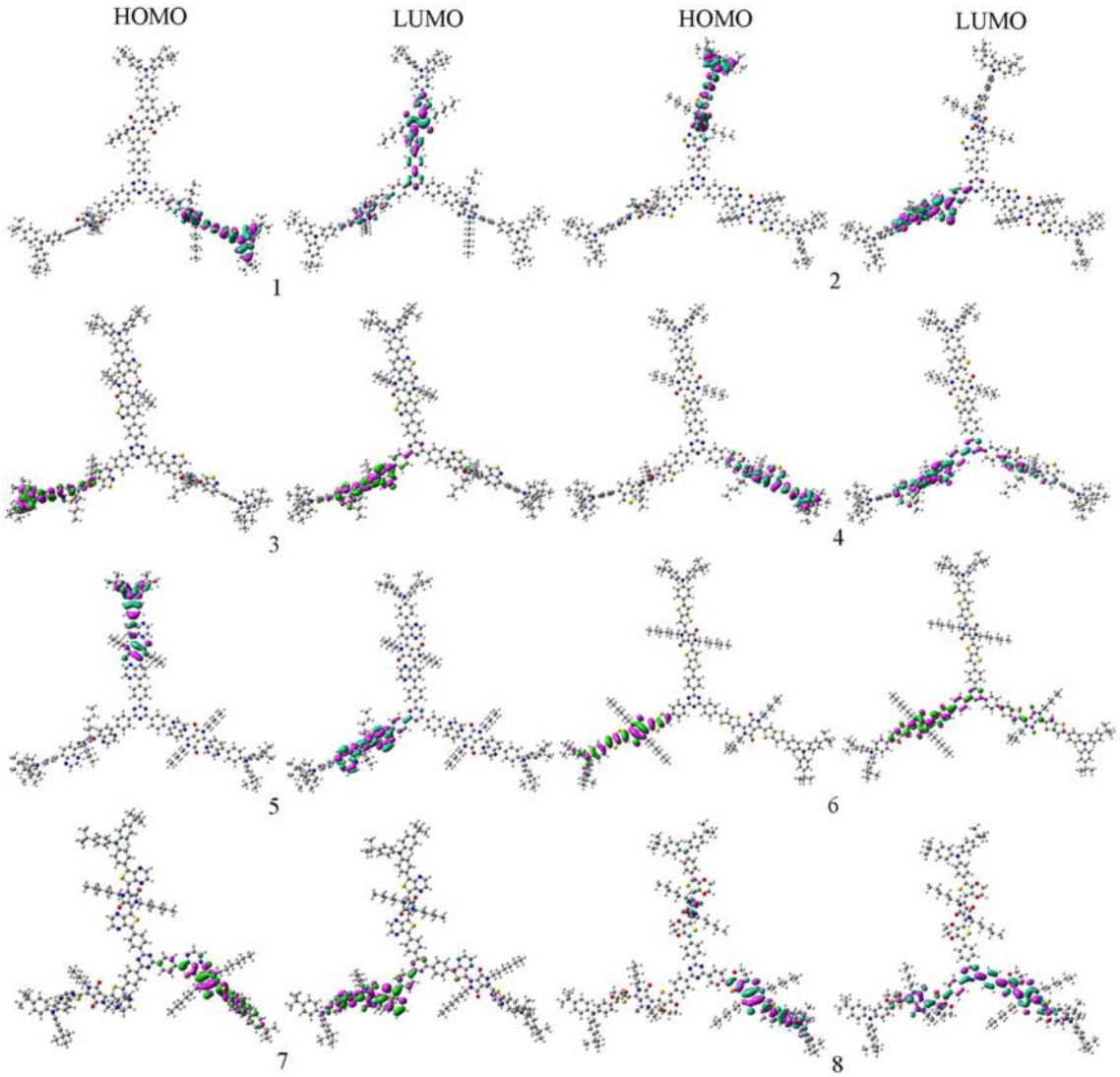

FIGURE 2 | The FMOs of the designed molecules at the PBE0/6-31G(d,p) level.

It is noteworthy that the stability is the most important criteria to evaluate the nature of devices for OSCs. Generally, the absolute hardness (η) was applied to explore the stability of the materials. From a viewpoint of conceptual density functional theory, the η values of the designed molecules were calculated with the following equation (Cheung and Troisi, 2010):

$$\eta = \frac{1}{2}\left(\frac{\partial \mu}{\partial N}\right) = \frac{1}{2}\left(\frac{\partial^2 E}{\partial N^2}\right) = \frac{AIP - AEA}{2} \quad (3)$$

Here, μ and N correspond to the chemical potential and total electron number, respectively. The adiabatic ionization potential (AIP) is the energy difference between the cation radical specie and its neutral specie, while the adiabatic electron affinity (AEA) represents the energy difference between the neutral molecule and its anion radical molecule.

RESULTS AND DISCUSSION

Frontier Molecular Orbitals and Band Gaps

In order to characterize the optical and electronic properties, we investigated the distributions of the FMOs for the designed molecules. The distribution of HOMOs and LUMOs are plotted in **Figure 2**. Based on Mulliken population analysis, molecular orbital contribution (%) from core TPTA, arms DPP, and end groups TPA to the FMOs of **1**–**8** are given in **Table 1**. The corresponding contributions (%) from TPTA, DPP, and TPA groups to the HOMOs-1 and LUMOs+1 of **1**–**8** are given in **Table S2**. As visualized in **Figure 2**, the distribution of HOMOs and LUMOs are spread over the conjugated backbone and show π orbital features. The HOMOs are mainly localized on the arm groups DPP and end groups TPA with only minor contributions from the core fragments TPTA. The sum contributions of DPP and TPA fragments are larger than 96.1%, while the

TABLE 1 | Molecular orbital contribution (%) from core TPTA, arms DPP, and end groups TPA to the FMOs of **1**–**8** at the PBE0/6-31G(d,p).

Species	HOMO			LUMO		
	TPTA	DPP	TPA	TPTA	DPP	TPA
1	0.7	32.5	66.4	17.8	79.4	2.8
2	0.6	34.5	64.9	8.3	88.4	3.3
3	0.3	18.3	81.4	8.4	88.5	3.1
4	0.8	53.7	45.5	17.2	80.9	2.0
5	0.3	29.8	69.9	8.4	89.	2.5
6	2.4	76.5	21.1	16.9	79.9	3.2
7	3.9	71.1	25.0	11.6	82.7	5.6
8	3.1	69.6	27.3	25.8	69.9	4.3

TPTA, 2,4,6-triphenyl-1,3,5-triazine moieties; DPP, diketopyrrolopyrrole moieties; TPA, triphenylamine moieties.

TABLE 2 | Calculated E_{HOMO}, E_{LUMO}, E_g, and ΔE_{L-L} (all in eV) for investigated molecules at the PBE0/6-31G(d,p).

Species	E_{HOMO}	E_{LUMO}	E_g	$\Delta E_{L\text{-}L}$[a]	$\Delta E_{L\text{-}L}$[b]
1	−5.04	−2.76	2.28	1.23	1.06
2	−5.07	−3.26	1.81	0.73	0.56
3	−5.03	−3.05	1.98	0.94	0.77
4	−5.02	−2.84	2.18	1.15	0.98
5	−5.02	−2.94	2.08	1.05	0.88
6	−4.86	−2.95	1.91	1.04	0.87
7	−4.80	−3.25	1.55	0.74	0.57
8	−4.69	−2.63	2.06	1.36	1.19

[a]*Energetic driving force for PCBM as donor.*
[b]*Energetic driving force for PC71BM as donor.*

corresponding values of TPTA fragments are within 3.9% for HOMOs. On the contrary, the LUMOs are mainly distributed on the DPP and TPTA moieties with minor contributions from TPA fragments. The sum contributions of DPP and TPTA fragments for LUMOs are larger than 94.4%, while the corresponding values of TPA fragments are within 5.6%. Obviously, the contributions of both DPP and TPTA fragments for LUMOs are larger than those of for HOMOs, respectively. The contributions of TPA fragments to LUMOs are decreased compared with those of to HOMOs, respectively. Similar phenomena are found for the HOMOs-1 and LUMOs+1 of **1**–**8**. The changes in contributions suggest that the electronic density flow from the end groups TPA to the arms groups DPP and cores groups TPTA for HOMOs → LUMOs excitations. This indicates that the end groups TPA serve as donors, whereas, the arm groups DPP and core groups TPTA serve as acceptors, respectively.

It is worth noting that the E_{HOMO}, E_{LUMO}, E_g, and ΔE_{L-L} are strongly related to the optical and electronic properties. The calculated values of E_{HOMO}, E_{LUMO}, E_g, and ΔE_{L-L} of the designed molecules are given in **Table 2** and depicted in **Figure 3**. As shown in **Figure 3**, it is clear that the E_{HOMO} values of **3**–**8** increase, while the corresponding value of **2** decreases compared with that of **1**. The E_{HOMO} values is in the order

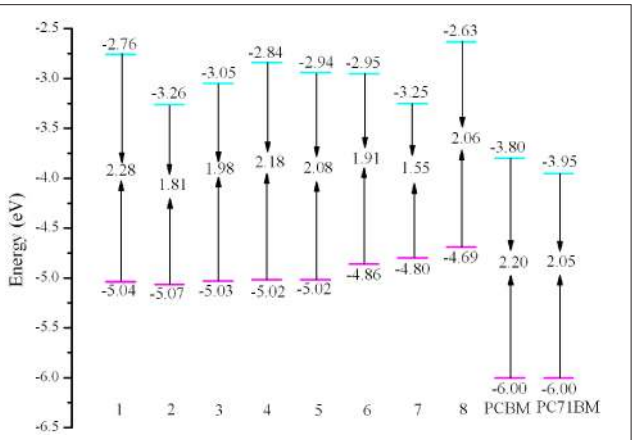

FIGURE 3 | Evaluation of calculated FMO energies for the designed molecules as well as FMO energies for PCBM and PC70BM at the PBE0/6-31G(d,p) level.

of **8** > **7** > **6** > **4** ≈ **5** > **3** > **1** > **2**. On the other hand, the E_{LUMO} values of **2**–**7** decrease, while the corresponding value of **8** increases compared with that of **1**. The sequence of E_{LUMO} values is **8** > **1** > **4** > **5** > **6** > **3** > **2** > **7**. Therefore, the E_g values of **2**–**8** decrease compared with that of **1**. The E_g values are in the order of **1** < **4** < **5** < **8** < **3** < **6** < **2** < **7**. The analysis indicates that the decrease of E_g is mainly attributable to the increased E_{HOMO} and declined E_{LUMO}. The reducing the E_g of the designed molecules should leads to bathochromic shifts of the maximum absorption compared with that of **1**. Consequently, the introduction of different groups to the side of DPP molecules backbones in the star-shaped molecules can tune the FMOs energy and E_g values of the original molecule. It provides a powerful strategy for design high-performance and desirable donor novel SMs. Furthermore, in order to ensure efficient charge transfer, the ΔE_{L-L} values must exceed the binding energy (0.2 ∼ 1.0 eV) (Hill et al., 2000; Knupfer, 2003). From **Table 2**, it is noteworthy that the ΔE_{L-L} values of the designed molecules are all beyond the binding energy with regard to PCBM and PC71BM as acceptors. It is clear that the sequence of the values of ΔE_{L-L} with regard to PCBM and PC71BM are all **8** > **1** > **4** > **5** > **6** > **3** > **7** > **2**. In addition, the differences between the E_{HOMO} of **1**–**8** and the E_{LUMO} of PCBM and PC71BM are larger than 0.73 and 0.56 eV, respectively. Thus, it is quite clear that the designed molecules can provide match well with PCBM and PC71BM as acceptors.

Absorption Spectra

The absorption wavelengths λ_{abs} (in nm), the oscillator strength *f*, and main assignments (coefficient), and the absorption region *R* of **1**–**8** at the PBE0/6-31G(d,p) level are listed in **Table 3**. *R* denotes for the difference of the longest and shortest wavelength values with oscillator strength larger than 0.01 considering the first 15 excited states (see **Table S3**). The simulated absorption spectra of **1**–**8** are shown in **Figure 4**, which were plotted by

TABLE 3 | The electronic transition, absorption wavelengths λ_{abs} (in nm), the oscillator strength *f*, main assignments (coefficient), and the absorption region *R* of **1**–**8** at the TD-PBE0/6-31G(d,p)//PBE0/6-31G(d,p) level, along with available experimental data.

Species	λ_{abs}	*f*	Assignment	*R*
1	543.4	1.79	H → L (0.12) H-2 → L (0.50) H-1 → L (0.20)	72.2
2	686.4	1.30	H-2 → L (0.66) H-5 → L (−0.17)	142.2
3	626.4	1.37	H → L (0.59) H → L+2 (0.21) H-2 → L+1 (0.21)	155.3
4	569.5	1.79	H → L (0.30) H-1 → L (0.43) H-1 → L+2 (−0.22)	82.3
5	597.2	1.01	H-2 → L (0.64) H-5 → L (0.23)	106.1
6	648.0	3.13	H → L (0.60) H → L+2 (0.21) H-2 → L+1 (−0.19)	139.1
7	799.6	2.19	H → L (0.24) H-2 → L (0.45) H → L+1 (−0.41)	225.7
8	602.4	2.83	H → L (0.51) H-2 → L (0.20), H-2 → L+1 (0.30)	152.7
Exp	523			

*Exp, Experimental results of **1** in thin film were taken from Sharma et al. (2014), Shiau et al. (2015).*

using the GaussSum 1.0 program (O'Boyle and Vos, 2003). As expected, the results displayed in **Table 3** reveals that the λ_{abs} of **2**–**8** exhibit bathochromic shifts compared with that of **1**. The bathochromic shifts values of **2**–**8** are 143, 83, 26.1, 53.8, 104.6, 256.2, and 59.0 nm (3834, 2439, 844, 1658, 2971, 5897, and 1803 cm^{-1}), respectively. Moreover, the λ_{abs} values are in the order of **7** > **2** > **6** > **3** > **8** > **5** > **4** > **1**, which is in excellent agreement with the corresponding reverse sequence of their E_g values. It reveals that the introduction of different groups to the side of DPP molecules backbones leads to bathochromic shifts of the maximum absorption for the original molecule. The order of the bathochromic shifts values compared with that of **1** is thieno[3,4-b]pyrazine (**7**) > benzo[c][1,2,5]thiadiazole (**2**) > thieno[3,2-b]thiophene (**6**) > benzo[c]isothiazole (**3**) > 2,3-dihydrothieno[3,4-b][1,4]dioxine (**8**) > quinoxaline (**5**) > benzo[c]thiophene (**4**). Additionally, one can find that **6**–**8** have larger oscillator strengths, while the corresponding values of **2**, **3**, and **5** possess slightly < that of **1**. The oscillator strength value of **4** is almost equal to that of **1**, indicating that the designed molecules shown large absorption intensity. At the same time, the designed molecules have large absorption region *R* (82.3–225.7 nm). The *R* values of 2–8 are larger than that of parent compound 1. It suggests that the introduction of different groups to the side of DPP molecules backbones lead to the increase of R values compared with parent molecule 1. The order of *R* values compared with that of **1** is thieno[3,4-b]pyrazine (**7**) > benzo[c]isothiazole (**3**) > 2,3-dihydrothieno[3,4-b][1,4]dioxine (**8**) > benzo[c][1,2,5]thiadiazole (**2**) > thieno[3,2-b]thiophene (**6**) > quinoxaline (**5**) > benzo[c]thiophene (**4**). It is noticeable that a good overlap between the absorption spectrum of the designed molecules and the solar emission spectrum, which can improve the light-absorption efficiency. It clearly shows that the introduction of different groups can extend the absorption spectrum toward longer wavelengths, which is beneficial to harvest more sunlight. These results imply that the designed compounds have strong absorption and are expected to be the promising candidates for donor materials in OSCs applications.

The calculated λ_{abs}, *f*, and main assignments (coefficient) of **1**–**8** at the B3LYP/6-31G(d,p) level are listed in **Table S4**. Comparing the results shown in **Table 3** with **Table S4**, one can find that the calculated λ_{abs} values of **1**–**8** at the B3LYP/6-31G(d,p) are larger than those obtained at the PBE0/6-31G(d,p), respectively. The differences between λ_{abs} at the B3LYP/6-31G(d,p) and PBE0/6-31G(d,p) levels are about 30 ∼ 50 nm. It should be mentioned that although the E_{HOMO} and E_{LUMO} are overestimated with both the PBE0 and B3LYP functionals, the predicted λ_{abs} values using PBE0 are found to be closer to the experimental findings. The trend for λ_{abs} at B3LYP/6-31G(d,p) is similar to using PBE0/6-31G(d,p) method. Obviously, B3LYP functional underestimate the E_g value, resulting in the large λ_{abs} compared with experimental value. Considering the FMOs energy levels and the predicted absorption spectra mentioned above, the PBE0/6-31G(d,p) approach is the best choice to well reproduce the experimental results. Therefore, the λ, η, *AIP*, and *AEA* of the designed molecules were computed at PBE0/6-31G(d,p).

Adiabatic Ionization Potential and Electron Affinity

It is well known that *AIP* and *AEA* are two major parameters that determine the charge transfer behavior for materials. The carrier polarity of materials can be adjusted by the *AIP* and *AEA* values (Chen and Chao, 2005; Liu et al., 2010). The lower *AIP* and higher *AEA* revealed that material would be better hole and electron transporter, respectively (Li et al., 2012). The calculated *AIP* and *AEA* of **1**–**8** are collected in **Table 4**. Obviously, the results displayed in **Table 4** show that the increasing sequence of *AIP* values is **8** < **7** < **6** < **4** < **5** < **1** < **3** < **2**. On the other hand, the decreasing order of *AEA* values is **7** > **2** > **3** > **6** > **5** > **4** > **1** > **8**. It indicates that the introduction of benzo[c]thiophene (**4**), quinoxaline (**5**), thieno[3,2-b]thiophene (**6**), and thieno[3,4-b]pyrazine (**7**) groups can decrease/increase *AIP*/*AEA* values compared with that of **1**. However, the benzo[c][1,2,5]thiadiazole (**2**) and benzo[c]isothiazole (**3**) groups can increase both *AIP* and *AEA* values, whereas 2,3-dihydrothieno[3,4-b][1,4]dioxine (**8**) group can decrease both *AIP* and *AEA* values compared with that of **1**. It is noticeable that the introduction of different aromatic heterocyclic group to the side of DPP molecules backbones can affect the *AIP* and *AEA* of the designed molecules.

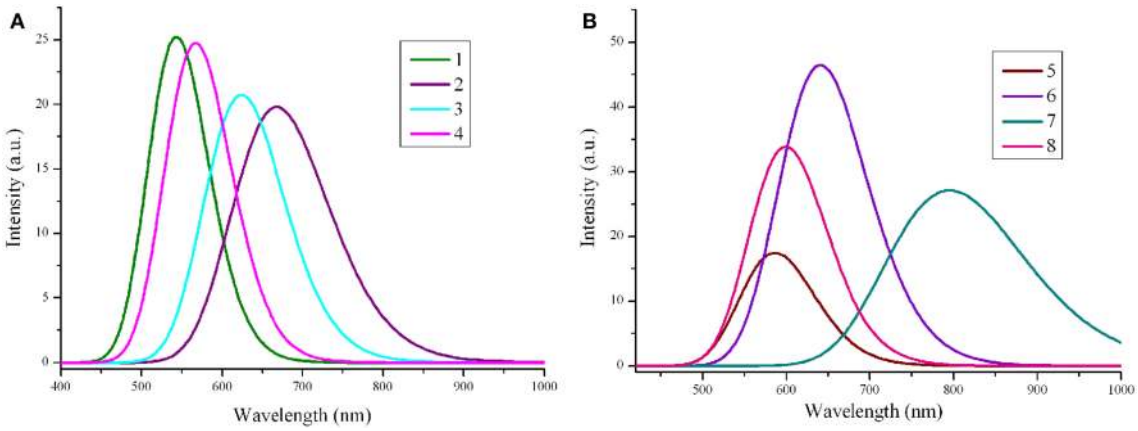

FIGURE 4 | The calculated absorption spectra of the investigated molecules (value of full width at half maximum is 3,000 cm^{-1}). **(A)** Molecules **1**–**4**; **(B)** Molecules **5**–**8**.

TABLE 4 | Calculated molecular *AIP* and *AEA* (both in eV) of **1**–**8** at the PBE0/6-31G(d,p) level.

Species	*AIP*	*AEA*
1	5.404	1.953
2	5.435	2.372
3	5.406	2.272
4	5.362	1.979
5	5.378	2.068
6	5.209	2.196
7	5.163	2.449
8	5.048	1.781

TABLE 5 | Calculated molecular λ_e, λ_h, and η (all in eV) of **1**–**8** at the PBE0/6-31G(d,p) level.

Species	λ_h	λ_e	η
1	0.054	0.134	1.725
2	0.058	0.112	1.532
3	0.046	0.209	1.567
4	0.090	0.135	1.692
5	0.051	0.138	1.655
6	0.107	0.091	1.506
7	0.129	0.122	1.357
8	0.128	0.128	1.633

Reorganization Energies and Stability Properties

The calculated λ_e, λ_h, and η of **1**–**8** are listed in **Table 5**. It is worth noting that the lower the reorganization energy values can be beneficial to the higher charge transfer rate (Marcus, 1964, 1993). Usually, tris(8-hydroxyquinolinato)aluminum(III) (Alq3, $\lambda_e = 0.276$ eV) and N,N′-diphenyl-N,N′-bis(3- methlphenyl)-(1,1′-biphenyl)-4,4′-diamine (TPD, $\lambda_h = 0.290$ eV) are taken as typical electron and hole transport materials, respectively (Gruhn et al., 2002; Lin et al., 2005). It is clear from **Table 5** that the λ_h values of **1**–**8** (0.046–0.129 eV) are smaller than that of TPD. It indicates that the hole transfer rates of **1**–**8** are higher than that of TPD. On the other hand, the λ_e values of **1**–**8** (0.091–0.209 eV) are smaller than that of Alq3. It implies that the electron transfer rates of **1**–**8** might be higher than that of Alq3. The λ_h values of **1**–**5** are slightly smaller than those of **6**–**8**, suggesting that the hole transfer rates of **1**–**5** should be higher than those of **6**–**8**, respectively. It indicates that the introduction of benzene (**1**), benzo[c][1,2,5]thiadiazole (**2**), benzo[c]isothiazole (**3**), benzo[c]thiophene (**4**), and quinoxaline (**5**) groups may lead to higher charge transfer rates than that of thieno[3,2-b]thiophene (**6**), thieno[3,4-b]pyrazine (**7**), and 2,3-dihydrothieno[3,4-b][1,4]dioxine (**8**) groups, respectively. The λ_e values is in the order of **3** > **5** > **4** > **1** > **8** > **7** > **2** > **6**. It suggests that molecules with benzo[c][1,2,5]thiadiazole (**2**), thieno[3,2-b]thiophene (**6**), thieno[3,4-b]pyrazine (**7**), and 2,3-dihydrothieno[3,4-b][1,4]dioxine (**8**) possess higher electron transfer rates, while molecules with benzo[c]isothiazole (**3**), benzo[c]thiophene (**4**), and quinoxaline (**5**) groups have lower electron transfer rates compared with that of **1**, respectively. Additionally, the λ_h values of **1**–**5** are smaller than those of their λ_e values, suggesting that the carrier mobility of the hole is larger than that of the electron. However, the λ_e values of **6** and **7** are smaller than those of their λ_h values, implying that the carrier mobility of the electron is larger than that of the hole. Moreover, the differences between λ_e and λ_h values of the designed molecules are in the region of 0.00 ∼ 0.087 eV except the corresponding value of **3** is 0.163 eV, respectively. It indicates that they exhibit better equilibrium feature for hole and electron transport. Therefore, **1**, **2**, and **4**–**8** are expected to be the promising candidates for ambipolar charge transports materials, whereas **3** can be used as hole and electron transport material.

The absolute hardness η of **1**–**8** were calculated and shown in **Table 5**. The η values is in the order of **1** > **4** > **5** > **8** > **3** > **2** > **6** > **7**. Inspection of **Table 5** reveals clearly that the η values of

2–**8** are smaller slightly than the value of **1**, which may be owing to the steric hindrances of the heterocyclic groups introduced to the side of DPP backbones in star-shaped DPP-based molecules. It implies that the introduction of different heterocyclic groups do not significantly affect the stability of the designed molecules.

CONCLUSION

In this contribution, a series of novel star-shaped molecules have been systematically investigated. Their electronic, optical, and charge transport properties studied using DFT and TD-DFT approaches. The calculated results show that the introduction of different groups to the side of DPP backbones in the star-shaped molecules can tune the FMOs energy and E_g values of the original molecule. The designed molecules can provide match well with PCBM and PC71BM as acceptors. Additionally, the λ_{abs} of **2**–**8** show bathochromic shifts compared with that of the original molecule **1**, respectively. The introduction of different groups can extend the absorption spectrum toward longer wavelengths, which is beneficial to harvest more sunlight. Our results suggest that the designed molecules are expected to be the promising candidates for ambipolar charge transport materials except molecule with benzo[c]isothiazole group (**3**) can be used as hole and electron transport material. Moreover, the different substituent groups do not significantly affect the stability of the designed molecules.

AUTHOR CONTRIBUTIONS

RJ conceived and designed the research and headed, wrote, and revised the manuscript. XZ contributed to the performance and analysis of the frontier molecular orbitals, absorption spectra the reorganization energies. Both authors contributed to manuscript revision, read, and approved the submitted version.

ACKNOWLEDGMENTS

This work was supported by NSFC (No. 21563002) and the Research Program of Sciences at Universities of Inner Mongolia Autonomous Region (No. NJZY19223).

SUPPLEMENTARY MATERIAL

The Supplementary Material for this article can be found online at: https://www.frontiersin.org/articles/10.3389/fchem.2019.00122/full#supplementary-material

REFERENCES

Abbotto, A., Seri, M., Dangate, M. S., De Angelis, F., Manfredi, N., Mosconi, E., et al. (2012). A vinylene-linked benzo[1,2-b:4,5-b′]dithiophene-2,1,3-benzothiadiazole low-bandgap polymer. *J. Polym. Sci. Pol. Chem.* 50, 2829–2840. doi: 10.1002/pola.26046

Adamo, C., and Barone, V. (1999). Toward reliable density functional methods without adjustable parameters: the PBE0 model. *HJ. Chem. Phys.* 110, 6158–6170. doi: 10.1063/1.478522

Bin, H., Yang, Y., Zhang, Z. G., Ye, L., Ghasemi, M., Chen, S., et al. (2017). 9.73% efficiency nonfullerene all organic small molecule solar cells with absorption-complementary donor and acceptor. *J. Am. Chem. Soc.* 139, 5085–5094. doi: 10.1021/jacs.6b12826

Blouin, N., Michaud, A., Gendron, D., Wakim, S., Blair, E., Neagu-Plesu, R., et al. (2008). Toward a rational design of poly(2,7-carbazole) derivatives for solar cells. *J. Am. Chem. Soc.* 130, 732–742. doi: 10.1021/ja0771989

Chandrasekharam, M., Anil Reddy, M., Ganesh, K., Sharma, G. D., Singh, S. P. J., and Rao, L. (2014). Synthesis and photovoltaic properties of D-A-D type small molecules containing diketopyrrolopyrrole (DPP) acceptor central unit with different donor terminal units. *Org. Electron.* 15, 2116–2125. doi: 10.1016/j.orgel.2014.05.033

Chaudhry, A. R., Muhammad, S., Irfan, A., Al-Sehemi, A. G., Haq, B. U., and Hussain, S. (2018). Structural, electronic, and nonlinear optical properties of novel derivatives of 9,12-diiodo-1,2-dicarba-closo-dodecaborane: density functional theory approach. *Z. Naturforsch. A* 73, 1037–1045. doi: 10.1515/zna-2018-0123

Chen, H. Y., and Chao, I. (2005). Effect of perfluorination on the charge-transport properties of organic semiconductors: density functional theory study of perfluorinated pentacene and sexithiophene. *Chem. Phys. Lett.* 401, 539–545. doi: 10.1016/j.cplett.2004.11.125

Chen, Y., Wan, X., and Long, G. (2013). High performance photovoltaic applications using solution-processed small molecules. *Acc. Chem. Res.* 46, 2645–2655. doi: 10.1021/ar400088c

Cheung, D. L., and Troisi, A. (2010). Theoretical study of the organic photovoltaic electron acceptor PCBM: morphology, electronic structure, and charge localization. *J. Phys. Chem. C* 114, 20479–20488. doi: 10.1021/jp1049167

Coughlin, J. E., Henson, Z. B., Welch, G. C., and Bazan, G. C. (2014). Design and synthesis of molecular donors for solution-processed high-efficiency organic solar cells. *Acc. Chem. Res.* 47, 257–270. doi: 10.1021/ar400136b

Dutta, P., Yang, W., Eom, S. H., Lee, W. H., Kang, I. N., and Lee, S. H. (2012). Development of naphtho[1,2-b:5,6-b′]dithiophene based novel small molecules for efficient bulk-heterojunction organic solar cells. *Chem. Commun.* 48 573–575. doi: 10.1039/C1CC15465F

Feng, H. F., Fu, W. F., Li, L., Yu, Q. C., Lu, H., Wan, J. H., et al. (2014). Triphenylamine modified bis-diketopyrrolopyrrole molecular donor materials with extended conjugation for bulk heterojunction solar cells. *Org. Electron.* 15, 2575–2586. doi: 10.1016/j.orgel.2014.07.020

Frisch, M. J., Trucks, G. W., Schlegel, H. B., Scuseria, G. E., Robb, M. A., Cheeseman, J. R., et al. (2009). *Gaussian 09*. Wallingford, CT: Gaussian, Inc.

Fujii, M., Shin,W., Yasuda, T., and Yamashita, K. (2016). Photon-absorbing charge-bridging states in organic bulk heterojunctions consisting of diketopyrrolopyrrole derivatives and PCBM. *Phys. Chem. Chem. Phys.* 18, 9514–9523. doi: 10.1039/C5CP06183K

Gruhn, N. E., da Silva Filho, D. A., Bill, T. G., Malagoli, M., Coropceanu, V., Kahn, A., et al. (2002). The vibrational reorganization energy in pentacene: molecular influences on charge transport. *J. Am. Chem. Soc.* 124, 7918–7919. doi: 10.1021/ja0175892

Guo, Y. Q., Wang, Y., Song, L. C., Liu, F., Wan, X., Zhang, H., et al. (2017). Small molecules with asymmetric 4-alkyl-8-alkoxybenzo[1,2-*b*:4,5-*b*′]dithiophene as the central unit for high-performance solar cells with high fill factors. *Chem. Mater.* 29, 3694–3703. doi: 10.1021/acs.chemmater.7b00642

He, C., He, Q. G., Yang, X. D., Wu, G. L., Yang, C. H., Bai, F. L., et al. (2007). Synthesis and photovoltaic properties of a solution-processable organic molecule containing triphenylamine and DCM moieties. *J. Phys. Chem. C* 111, 8661–8666. doi: 10.1021/jp070714x

Hill, I. G., Kahn, A., Soos, Z. G., and Pascal, R. A Jr. (2000). Charge-separation energy in films of π-conjugated organic molecules. *Chem. Phys. Lett.* 327, 181–188. doi: 10.1016/S0009-2614(00)00882-4

Irfan, A., Assiri, M., and Al-Sehemi, A. G. (2018). Exploring the optoelectronic and charge transfer performance of diaza[5]helicenes at molecular and bulk level. *Org. Electron.* 57, 211–220. doi: 10.1016/j.orgel.2018.03.022

Irfan, A., Muhammad, S., Chaudhry, A. R., Al-Sehemi, A. G., and Jin, R. (2017). Tuning of optoelectronic and charge transport properties in star shaped anthracenothiophene-pyrimidine derivatives as multifunctional materials. *Optik* 149, 321–331. doi: 10.1016/j.ijleo.2017.09.065

Jeon, I., Delacou, C., Nakagawa, T., and Yutaka Matsuo, Y. (2016). Enhancement of open-circuit voltage by using the 58-p silylmethyl fullerenes in small-molecule organic solar cells. *Chem. Asian J.* 11, 1268–272. doi: 10.1002/asia.201501400

Jin, R. (2015). Theoretical study of the optical and charge transport properties of star-shaped molecules with 1,3,5-triazine-core derivatives as organic light-emitting and organic solar cells materials. *C. R. Chimie.* 18, 954–959. doi: 10.1016/j.crci.2015.05.021

Jin, R., and Irfan, A. (2015). Theoretical study on photophysical properties of multifunctional star-shaped molecules with 1,8-naphthalimide core for organic light-emitting diode and organic solar cell application. *Theor. Chem. Acc.* 134:89. doi: 10.1007/s00214-015-1693-8

Jin, R., and Xiao, W. (2015). Rational design of organoboron heteroarene derivatives as luminescent and charge transport materials for organic light-emitting diodes. *New J. Chem.* 39, 8188–8194. doi: 10.1039/C5NJ01499A

Kan, B., Li, M., Zhang, Q., Liu, F., Wan, X., Wang, Y., et al. (2015). A series of simple oligomer-like small molecules based on oligothiophenes for solution-processed solar cells with high efficiency. *J. Am. Chem. Soc.* 137, 3886–3893. doi: 10.1021/jacs.5b00305

Knupfer, M. (2003). Exciton binding energies in organic semiconductors. *Appl. Phys. A* 77, 623–626. doi: 10.1007/s00339-003-2182-9

Köse, M. E., Mitchell, W. J., Kopidakis, N., Chang, C. H., Shaheen, S. E., Kim, K., et al. (2007). Theoretical studies on conjugated phenyl-cored thiophene dendrimers for photovoltaic applications. *J. Am. Chem. Soc.* 129, 14257–14270. doi: 10.1021/ja073455y

Ku, J., Lansac, Y., and Jang, Y. H. (2011). Time-dependent density functional theory study on benzothiadiazole-based low-band-gap fused-ring copolymers for organic solar cell applications, *J. Phys. Chem. C* 115, 21508–21516. doi: 10.1021/jp2062207

Lee, C., Yang, W., and Parr, R. G. (1988). Development of the colle–salvetti correlation-energy formula into a functional of the electron density. *Phys. Rev. B* 37, 785–789. doi: 10.1103/PhysRevB.37.785

Lenes, M., Wetzelaer, G. -J. A. H., Kooistra, F. B., Veenstra, S. C., Hummelen, J. C., and Blom, P. W. M. (2008). Fullerene bisadducts for enhanced open-circuit voltages and efficiencies in polymer solar cells. *Adv. Mater.* 20, 2116–2119. doi: 10.1002/adma.200702438

Li, G., Zhu, R., and Yang, Y. (2012). Polymer solar cells. *Nat. Photonics.* 6, 153–161. doi: 10.1038/nphoton.2012.11

Lin, B. C., Cheng, C. P., You, Z. Q., and Hsu, C. P. (2005). Charge transport properties of tris(8-hydroxyquinolinato)aluminum(III): why it is an electron transporter. *J. Am. Chem. Soc.* 127, 66–67. doi: 10.1021/ja045087t

Lin, Y., and Zhan, X. (2016). Oligomer molecules for efficient organic photovoltaics. *Acc. Chem. Res.* 49, 175–183. doi: 10.1021/acs.accounts.5b00363

Lin, Y. Z., Ma, L. C., Li, Y. F., Liu, Y. Q., Zhu, D. B., and Zhan, X. W. (2013). A solution-processable small molecule based on benzodithiophene and diketopyrrolopyrrole for high-performance organic solar cells. *Adv. Energy. Mater.* 3, 1166–1170. doi: 10.1002/aenm.201300181

Liu, C. C., Mao, S. W., and Kuo, M. Y. (2010). Cyanated pentaceno[2,3-*c*]chalcogenophenes for potential application in air-stable ambipolar organic thin-film transistors. *J. Phys. Chem. C* 114, 22316–22321. doi: 10.1021/jp1099464

Loser, S., Lou, S. J., Savoie, B. M., Bruns, C. J., Timalsina, A., Leonardi, M. J., et al. (2017). Systematic evaluation of structure–property relationships in heteroacene–diketopyrrolopyrrole molecular donors for organic solar cell. *J. Mater. Chem. A* 5, 9217–9232. doi: 10.1039/C7TA02037F

Maglione, C., Carella, A., Centore, R., Chávez, P., Lévêque, P., Fall, S., et al. (2017). Novel low bandgap phenothiazine functionalized DPP derivatives prepared by direct heteroarylation: application in bulk heterojunction organic solar cells. *Dyes. Pigments.* 141, 169–178. doi: 10.1016/j.dyepig.2017.02.012

Marcus, R. A. (1964). Chemical and electrochemical electron-transfer theory. *Annu. Rev. Phys. Chem.* 15, 155–196.

Marcus, R. A. (1993). Electron transfer reactions in chemistry. theory and experiment. *Rev. Mod. Phys.* 65, 599–610.

Ni, D., Zhao, B., Shi, T., Ma, S., Tu, G., and Wu, H. (2013). Monodisperse low-bandgap macromolecule-based 5,5′-bibenzo[c][1,2,5]thiadiazole swivel cruciform for organic solar cells. *ACS. Macro. Lett.* 2, 621–624. doi: 10.1021/mz4002436

O'Boyle, N. M., and Vos, J. G. (2003). *GaussSum 1.0*. Dublin: Dublin City University.

Patra, D., Huang, T. Y., Chiang, C. C., Maturana, R. O., Pao, C. W., Ho, K. C., et al. (2013). 2-Alkyl-5-thienyl-substituted benzo[1,2-b:4,5-b]dithiophene-based donor molecules for solution-processed organic solar cells. *ACS Appl. Mater. Interfaces* 5, 9494–9500. doi: 10.1021/am4021928

Qu, S., and Tian, H. (2012). Diketopyrrolopyrrole (dpp)-based materials for organic photovoltaics. *Chem. Commun.* 48, 3039–3051. doi: 10.1039/c2cc17886a

Sancho-García, J. C. (2007). Assessment of density-functional models for organic molecular semiconductors: the role of Hartree–Fock exchange in charge-transfer processes. *Chem. Phys.* 331, 321–331. doi: 10.1016/j.chemphys.2006.11.002

Scharber, M. C., Wuhlbacher, D., Koppe, M., Denk, P., Waldauf, C., Heeger, A. J., et al. (2006). Design rules for donors in bulk-heterojunction solar cells-towards 10 % energy-conversion efficiency. *Adv. Mater.* 18, 789–794. doi: 10.1002/adma.200501717

Sharma, G. D., Zervaki, G. E., Angaridis, P. A., Kitsopoulos, T. N., and Coutsolelos, A. G. (2014). Triazine-bridged porphyrin triad as electron donor for solution-processed bulk hetero-junction organic solar cells. *J. Phys. Chem. C* 118, 5968–5977. doi: 10.1021/jp500090h

Shiau, S. Y., Chang, C. H., Chen, W. J., Wang, H. J., Jeng, R. J., and Lee, R. H. (2015). Star-shaped organic semiconductors with planar triazine core and diketopyrrolopyrrole branches for solution-processed small-molecule organic solar cells. *Dyes. Pigments* 115, 35–49. doi: 10.1016/j.dyepig.2014.12.007

Tawada, Y., Tsuneda, T., Yanagisawa, S., Yanai, T., and Hirao, K. (2004). A long-range-corrected time-dependent density functional theory. *J. Chem. Phys.* 120, 8425–8433. doi: 10.1063/1.1688752

Vala, M., Krajčovič, J., Luňák, Jr., S., Ouzzane, I., Bouillon, J. P., and Weiter, M. (2014). HOMO and LUMO energy levels of N,N′-dinitrophenyl-substituted polar diketopyrrolopyrroles (DPPs). *Dyes Pigments* 106, 136–142. doi: 10.1016/j.dyepig.2014.03.005

Wang, J. L., Liu, K. K., Liu, S., Xiao, F., Chang, Z. F., Zheng, Y. Q., et al. (2017). Donor end-capped hexafluorinated oligomers for organic solar cells with 9.3% efficiency by engineering the position of π-bridge and sequence of two-step annealing. *Chem. Mater.* 29, 1036–1046. doi: 10.1021/acs.chemmater.6b03796

Wazzan, N., El-Shishtawy, R. M., and Irfan, A. (2018). DFT and TD–DFT calculations of the electronic structures and photophysical properties of newly designed pyrene-core arylamine derivatives as hole-transporting materials for perovskite solar cells. *Theor. Chem. Acc.* 137:9. doi: 10.1007/s00214-017-2183-y

Wu, J., Kan, Y. -H., Wu, Y., and Su, Z. -M. (2013). Computational design of host materials suitable for green-(deep) blue phosphors through effectively tuning the triplet energy while maintaining the ambipolar property. *J. Phys. Chem. C* 117, 8420–8428. doi: 10.1021/jp4008174

Xiao, S., Stuart, A. C., Liu, S., Zhou, H., and You, W. (2010). Conjugated polymer based on polycyclic aromatics for bulk heterojunction organic solar cells: a case study of quadrathienonaphthalene polymers with 2% efficiency. *Adv. Funct. Mater.* 20, 635–643. doi: 10.1002/adfm.200901407

Yanai, T., Tew, D. P., and Handy, N. C. (2004). A new hybrid exchange–correlation functional using the coulomb-attenuating method (CAM-B3LYP). *Chem. Phys. Lett.* 393, 51–57. doi: 10.1016/j.cplett.2004.06.011

Yao, H., Ye, L., Zhang, H., Li, S., Zhang, S., and Hou, J. (2016). Molecular design of benzodithiophene-based organic photovoltaic materials. *Chem. Rev.* 116, 7397–7457. doi: 10.1021/acs.chemrev.6b00176

Zhang, G., and Musgrave, C. B. (2007). Comparison of DFT methods for molecular orbital eigenvalue calculations. *J. Phys. Chem. A* 111, 1554–1561. doi: 10.1021/jp061633o

Zhang, L., Pei, K., Yu, M., Huang, Y., Zhao, H., Zeng, M., et al. (2012). Theoretical investigations on donor-acceptor conjugated copolymers based on naphtha [1, 2-c: 5, 6-c] bis [1, 2, 5] thiadiazole for organic solar

cell applications. *J. Phys. Chem. C* 116, 26154–26161. doi: 10.1021/jp306656c

Zhang, Y. M., Tan, H., Xiao, M. J., Bao, X. C., Tao, Q., and Wang, Y. F. (2014). D–A–Ar-type small molecules with enlarged π-system of phenanthrene at terminal for high-performance solution processed organic solar cells. *Org. Electron.* 15, 1173–1183. doi: 10.1016/j.orgel.2014.03.011

Zhang, Z., Zhou, Z., Hu, Q., Liu, F., Russell, T. P., and Zhu, X. (2017). 1, 3-bis (thieno [3, 4-b] thiophen-6-yl)-4 H-thieno [3, 4-c] pyrrole-4, 6 (5 H)-dione-Based small-molecule donor for efficient solution-processed solar cells. *ACS Appl. Mater. Interfaces* 9, 6213–6219. doi: 10.1021/acsami.6b14572

Zhao, Y., and Truhlar, D. G. (2008). The M06 suite of density functionals for main group thermochemistry, thermochemical kinetics, noncovalent interactions, excited states, and transition elements: two new functionals and systematic testing of four M06-class functionals and 12 other functionals. *Theor. Chem. Acc.* 120, 215–241.

Zhou, H., Yang, L., and You, W. (2012). Rational design of high performance conjugated polymers for organic solar cells. *Macromolecules* 45, 607–632. doi: 10.1021/ma201648t

Conflict of Interest Statement: The authors declare that the research was conducted in the absence of any commercial or financial relationships that could be construed as a potential conflict of interest.